View metadata, citation and similar papers at core.ac.uk

brought to you by CORE

provided by Queen's University Research Portal

W-Band Planar Wide-Angle Scanning Antenna Architecture

Zelenchuk, D., Martinez-Ros, A., Zvolensky, T., Gomez-Tornero, J., Goussetis, G., Buchanan, N., ... Fusco, V. (2013). W-Band Planar Wide-Angle Scanning Antenna Architecture. Journal of Infrared, Millimeter, and Terahertz Waves, 34(2), 127-139. DOI: 10.1007/s10762-013-9960-z

Published in:
Journal of Infrared, Millimeter, and Terahertz Waves

Document Version:
Peer reviewed version

Queen's University Belfast - Research Portal:
Link to publication record in Queen's University Belfast Research Portal

General rights
Copyright for the publications made accessible via the Queen's University Belfast Research Portal is retained by the author(s) and / or other copyright owners and it is a condition of accessing these publications that users recognise and abide by the legal requirements associated with these rights.

Take down policy
The Research Portal is Queen's institutional repository that provides access to Queen's research output. Every effort has been made to ensure that content in the Research Portal does not infringe any person's rights, or applicable UK laws. If you discover content in the Research Portal that you believe breaches copyright or violates any law, please contact openaccess@qub.ac.uk.

Download date:16. Feb. 2017

The final publication is available at

link.springer.com

http://link.springer.com/article/10.1007/s10762-013-9960-z

DOI 10.1007/s10762-013-9960-z

Journal of Infrared, Millimeter, and Terahertz Waves

February 2013, Volume 34, Issue 2, pp 127-139

W-Band Planar Wide-Angle Scanning Antenna Architecture

- Dmitry Zelenchuk,
- Alejandro Javier Martinez-Ros,
- Tomas Zvolensky,
- Jose Luis Gomez-Tornero,
- George Goussetis,
- Neil Buchanan,
- David Linton,
- Vincent Fusco

W-band Planar Wide-angle Scanning Antenna Architecture

Abstract This paper proposes a hybrid scanning antenna architecture for applications in mm-wave intelligent mobile sensing and communications. We experimentally demonstrate suitable W-band leaky-wave antenna prototypes in substrate integrated waveguide (SIW) technology. Three SIW antennas have been designed that within a 6.5% fractional bandwidth provide beam scanning over three adjacent angular sectors. Prototypes have been fabricated and their performance has been experimentally evaluated. The measured radiation patterns have shown three frequency scanning beams covering angles from 11 to 56 degrees with beamwidth of 10±3 degrees within the 88-94GHz frequency range.

Keywords Millimeter-wave mobile sensing and communications· W-band antennas· Leaky wave antennas·

Introduction

Millimeter wave technology in recent years has become strongly associated with advances in intelligent sensing and communication applications such as automotive anti-collision systems [1–3], hazard detection and avoidance [4], autonomous landing guidance [5], satellite mobile multimedia service [6], and aircraft imagers [7]. Directive antennas emerge as a key component in most of these applications driven by the requirement to meet stringent link budget specifications and/or provide good imaging resolution. Many practical scenarios, (requiring e.g. continuous service when an obstacle blocks the line of sight, tracking of mobile terminals placed on a moving vehicle or scanning within a given field of view) further pose the need for antennas with beam-steering capabilities. Coupled with commercial viability constraints, the development of mm-wave directive antenna systems with beam-steering capabilities that also maintain compatibility with low-cost mass-manufacturing process and easy integration with the front-end has emerged as a key challenge for both communication and sensing applications [8, 9].

Despite the significant advantages of on-chip antennas in terms of ease of integration, compatibility with established fabrication techniques as well as volume and mass, their poor efficiency and strong unwanted coupling with the RF front-end is limiting their application beyond very short range systems [8]. Among the traditional in-package directive antenna solutions, phased arrays [10] involve a cumbersome feeding network which is impractical for mass-market mm-wave applications. Reflector and lens antenna architectures [11, 12], although compatible with a simpler feeding network, are bulky and typically require mechanical reconfiguration to perform beam scanning, adding significant complexity and cost, increase power consumption and significantly limiting the scanning speed.

The class of travelling-wave and leaky-wave antennas has emerged as a promising candidate for directive radiation emission from low profile conformable structures with simple feeding network [13–17]. These antennas offer significant complexity, cost and volume advantages for mm-wave sensing and communications applications when compared to phased arrays or reflector antenna architectures [18]. They can be implemented in either bulk micro-machined [13, 19–21] or planar PCB compatible [15, 22–24] technologies. Additionally, frequency beam scanning is an inherent feature in this class of antennas. This feature can be advantageous provided the required frequency range to perform a scan lies within a relatively narrow fractional bandwidth. Despite the research efforts concentrated on enhancing the frequency scanning of leaky wave antennas [19], the fractional bandwidth required for a full coverage remains in the order of 30%, which is too broad for many applications.

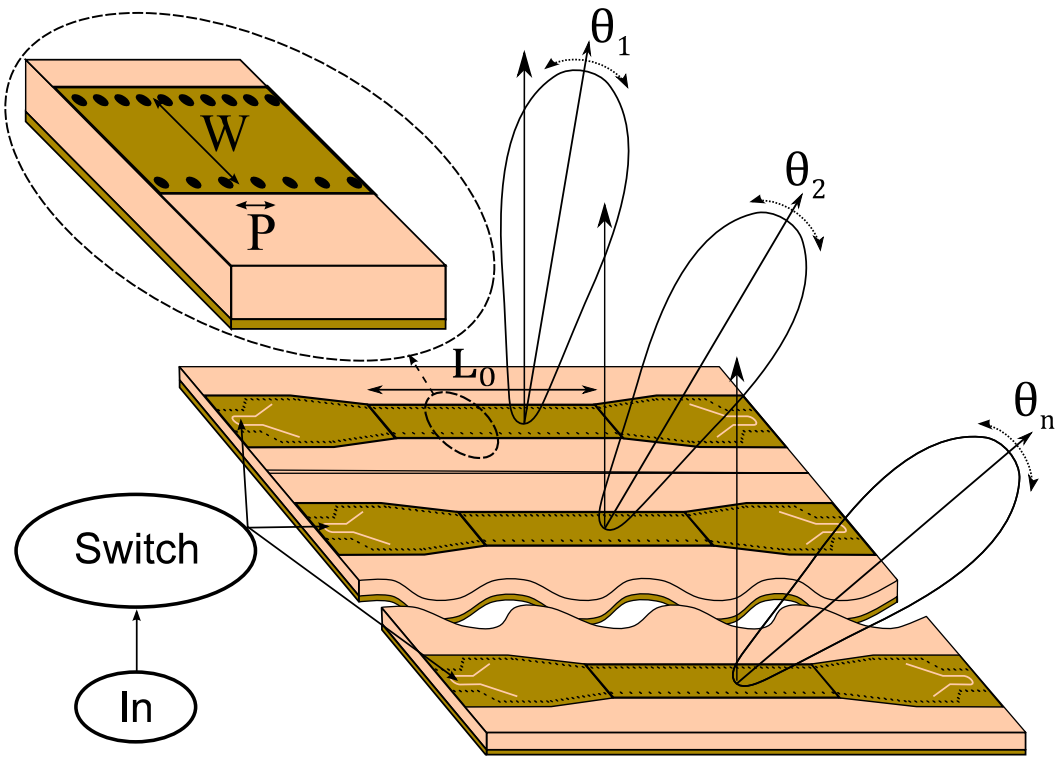

Fig. 1. Switch-beam leaky-wave antenna array scanning multiple sectors.

In order to overcome this problem, here we propose a sectorized leaky-wave antenna architecture that exploits a hybrid frequency-scanning switch-operated concept. The concept is schematically depicted in Fig. 1. An array of linear leaky-wave antennas (LWAs) is connected with the feeding network through a single-pole multiple-throw (SPMT) switch. Each LWA is designed to cover a given sector by frequency-scanning within a specified bandwidth. The sectors covered by successive antennas are complementary and the switch is employed to switch between those, so that full coverage can be obtained.

High-performance MMIC mm-wave switches are now routinely available – some of the authors have recently demonstrated examples in [25]. In order to optimize manufacturability and performance, SIW (substrate integrated waveguide) [26] is the preferred technology for the realization of the LWAs, which offers better tolerance and loss characteristics in comparison with other PCB compatible transmission lines such as microstrip and coplanar waveguide [27]. In this paper we therefore demonstrate the capability to design SIW LWAs suitable for the scanning antenna architecture of Fig. 1. Design challenges include the requirement to scan complementary sectors within a given 6.5% fractional bandwidth and with a similar beamwidth for all antennas. Experimental result for W-band SIW antenna prototypes are reported.

Design and simulations

The capability to realize LWAs with flexible control of the propagation constant in SIW technology has been demonstrated in [22] by means of Ku-band examples. The operating principle is based on a SIW (see Fig. 1), where one row of vias is sufficiently dense to operate as a fully reflecting sidewall [26], while the other row of vias is more sparse so that it performs as a partially reflecting sidewall [22]. The latter is exploited to control the excitation of an equivalent magnetic current at the edge of a parallel plate waveguide section, which radiates into free space. By adapting the separation of the two rows of vias, the width of the SIW (parameter W in Fig. 1) can be adjusted, which predominantly affects the phase constant and the pointing angle. Similarly, by increasing/reducing the separation between the vias in the sparse array (parameter P in Fig. 1), the magnitude of the radiating equivalent magnetic current can be reduced/increased and hence predominantly determine the leakage constant. Full-wave electromagnetic modeling can be used to decouple the two effects and the application of this technique in the design of LWAs with independent control of the beamwidth and the beam-pointing angle can be achieved [22].

Significantly, the design maintains compatibility with SIW technology and hence shares the advantages of high performance and easy in-package integration.

The design of an antenna system such as the one depicted in Fig. 1 commences by specifying the desired frequency band of operation, here assumed to be the frequency range between f_{min} and f_{max}. Subsequently, the required number of sectors for the given bandwidth as well as initial values for the width, W, for each angle sector antenna can be obtained using the dispersion of the fully shielded waveguide as a first approximation. For moderately small leakage rate, according to this approximation the beam pointing angle of a LWA is given by [28]:

$$\sin\theta_{rad} \approx \beta / k_0 \tag{1}$$

where $\beta = \sqrt{k^2 - k_c^2}$ is the longitudinal propagation constant and $k = k_0\sqrt{\varepsilon_r}$ the wavenumber associated with a waveguide filled with dielectric of relative permittivity ε_r. In the above k_0 is the free-space wavenumber [29]. Setting the angle $\theta_{n,rad}^{f\max}$ where the nth antenna is pointing at the maximum operation frequency, f_{max}, to be the maximum angle of coverage, the width, W, of the corresponding SIW can be obtained using equation (1) in conjunction with:

$$k_c = \frac{\pi}{W_{eff}\sqrt{\varepsilon_r}} \tag{2}$$

where the effective width is given by [30]

$$W_{eff} = W - 1.08\frac{d^2}{p} + 0.1\frac{d^2}{W}$$

For the obtained value of the nth SIW width, it is then possible to obtain the angle $\theta_{n,rad}^{f\min}$ where the nth antenna is pointing at the lowest operation frequency, f_{min}. This value is subsequently used for the angle $\theta_{n-1,rad}^{f\max}$ where the (n-1)th antenna is pointing at the maximum operation frequency, f_{max} and the process is repeated until the desired coverage is achieved. This process provides the number of sectors for the given frequency band as well as initial values for the width, W, of all LWA.

Initial values for the separation, P, between the sparse via row as well as the total length of each antenna can be obtained considering the beamwidth and radiation efficiency at the central operating frequency. The radiation efficiency is typically required to be high, so that a small fraction of the power entering each LWA reaches the other end [28]. The beamwidth is determined according to the application requirements and certainly to be commensurate with the scanning range. Once the beamwidth and efficiency are determined at the central operating frequency, the leakage rate and antenna length can be obtained using available design procedures [22, 31]. Additional optimization of the antenna structure is necessary to complete the design procedure, which can be done using either transverse resonance model [32] or full-wave simulations [22].

The above design procedure is here demonstrated by means of an example. The operating frequency for this example is in the range between f_{min}= 88 GHz and f_{max}= 94 GHz and the aim is to cover the angular range of 5°-55°. The substrate chosen for the antennas implementation is PTFE, 0.1mm thick with permittivity of 2.1 and the loss tangent of 0.0008. Using the synthesis procedure outlined above, it can be easily shown that the antenna system involves a 3 sector design, where the initial widths, W, of the three antennas can be found to be 1.18mm, 1.25mm, and 1.38mm. A beamwidth of approximately 10 degrees was chosen as sufficient to provide the resolution commensurate with this antenna architecture. Using the initial values of the waveguide widths and exploiting detailed analysis of the dispersion characteristics of the SIW with partially reflective wall [32], the dimensions of the radiating part of the antenna were optimized. The final dimensions for the three LWAs after optimization are gathered in Table 1.

Table 1. Parameters of the leaky wave antennas.

Nº	θ_{rad}	$\Delta\theta$	α/k_0	L_0/λ_0	L_0 (mm)	W(mm)	P(mm)
1	10º	10º	0.0316	5.8	18.5	1.16	0.6
2	30º	10º	0.0277	6.61	21.1	1.15	0.75
3	50º	10º	0.0205	8.91	28.4	1.19	0.9

Three antenna prototypes based on the parameters of Table 1 have been designed. In order to be compatible with the testing equipment, each antenna consists of three distinctive parts, as shown in Fig. 1: grounded coplanar waveguide (GCPW)-SIW transition; transition from SIW to LWA; and radiating part of LWA. The antennas are excited by grounded coplanar waveguide in order to provide an interface to the measurement instrument. A GCPW-SIW transition matches the structure to the instrument interface and an SIW-LWA transition is necessary to compensate and reduce mismatch between propagation constants in the transmission lines. The transitions can be designed assuming a non-radiating SIW and kept fixed for the various antenna prototypes.

The frequency scanning properties of the antennas as obtained from closed-form analysis of SIW waveguide and full-wave simulation of the optimized structures (CST Microwave Studio time domain solver) are presented in Fig. 2. As one can see for large elevation angles, the approximate estimation of the pointing angle based on the closed form expressions is in very good agreement with the full-wave results of the finite antennas. The agreement deteriorates for smaller elevation angles; this is attributed to the strong dispersion associated with waveguide operation close to cutoff [28].

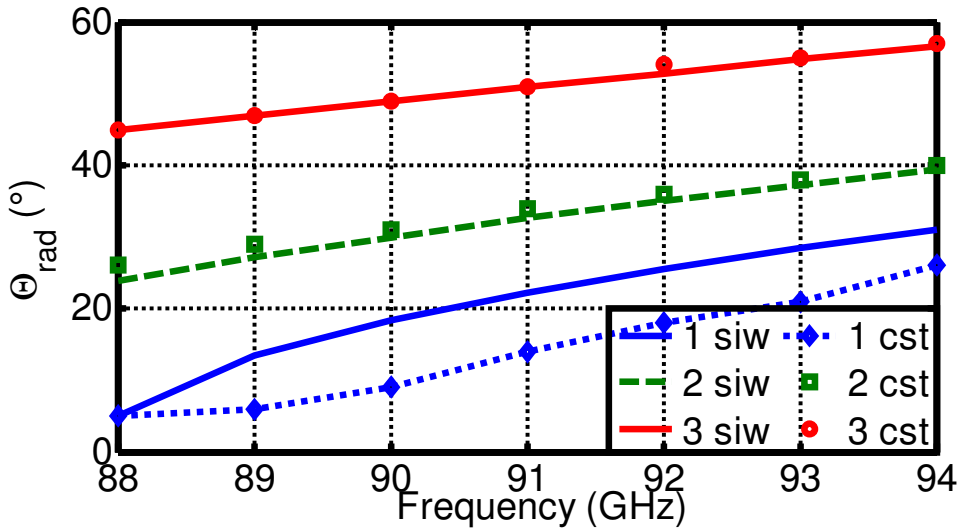

Fig. 2. Frequency beam scanning calculated with SIW formulas and for optimized structures with CST Microwave Studio.

The frequency-scanning response demonstrated in Fig. 2 is an easy mechanism to steer the beam in FMCW radar applications, and other radar or communication applications in which the signal bandwidth is narrow enough. It must also be considered that the frequency-sensitivity can be further controlled, by means of using different dielectric substrate or adding dispersion engineered circuits [19, 31]. Nevertheless, at W-band the absolute bandwidth without beam squint is quite large, due to the high frequencies involved. As shown in Fig. 2 the frequency-angle sensitivity is found to be 2.5deg/GHz which ensures that a signal with 100MHz bandwidth would barely notice any beam squint response.

The radiation patterns of each antenna as obtained from CST Microwave Studio are shown in Fig. 3, Fig. 4 and Fig. 5 respectively. Each antenna allows scanning within the designated sector. As shown in these figures, the beamwidth is largely constant and equal to 10° for angles away from broadside. Close to broadside, the design with θ_{rad}=10° does not preserve the narrow beamwidth below 91GHz, due to the increased leakage rates associated with waveguide operation close to cutoff [19, 28]. According to Figs. 3-5, within the proposed antenna architecture, the three antennas can cover angular sectors of 13°-55°. It is worth noting that within each selected angular subsector the gain variation with frequency does not exceed 1dB, except for the 1st antenna below 91GHz.

In order to demonstrate the whole radiation pattern of the SIW LWA a 3D radiation pattern of the first antenna calculated at 91GHz is presented in Fig. 6. The antenna is evidently a line-source antenna; the design produces the desired narrow beam in the scan plane, but the radiation pattern in the cross-plane is just a fan beam whose detailed beam shape depends on the cross-sectional dimensions of the leaky-wave antenna. This pattern is not unique and pertinent to practically any configurations of line-source leaky wave antennas.

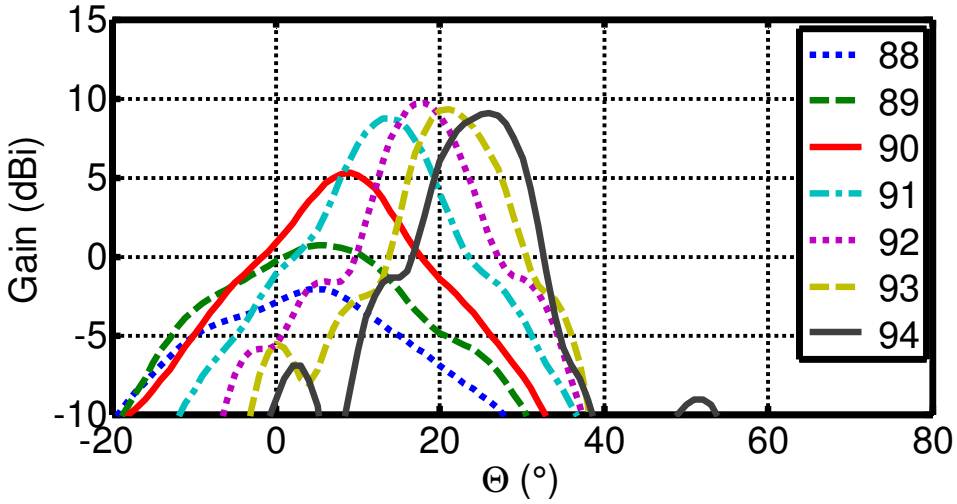

Fig. 3. Simulated radiation pattern of 1st LWA.

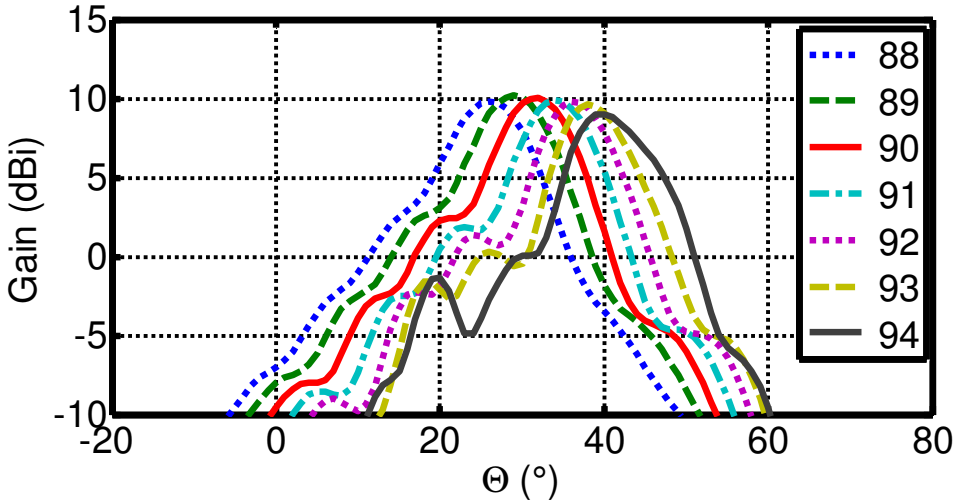

Fig. 4. Simulated radiation pattern of 2nd LWA.

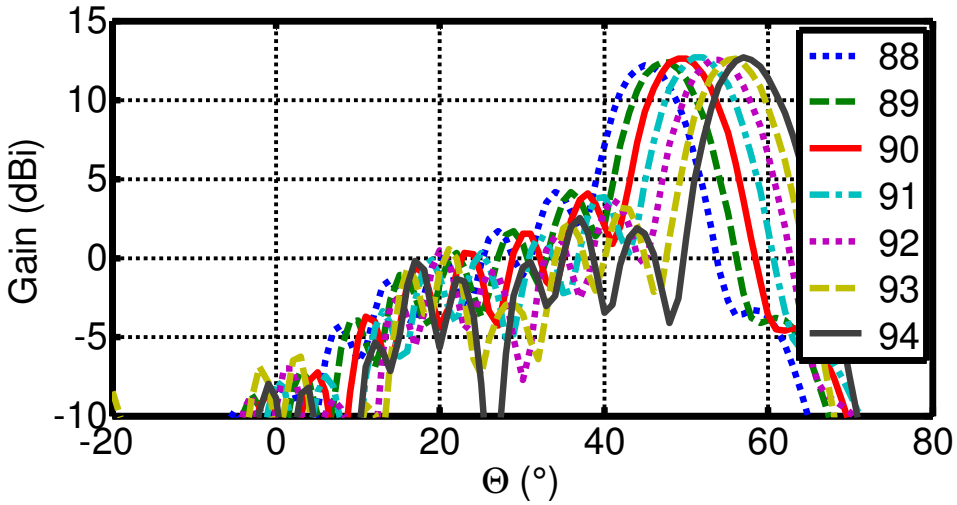

Fig. 5. Simulated radiation pattern of 3rd LWA.

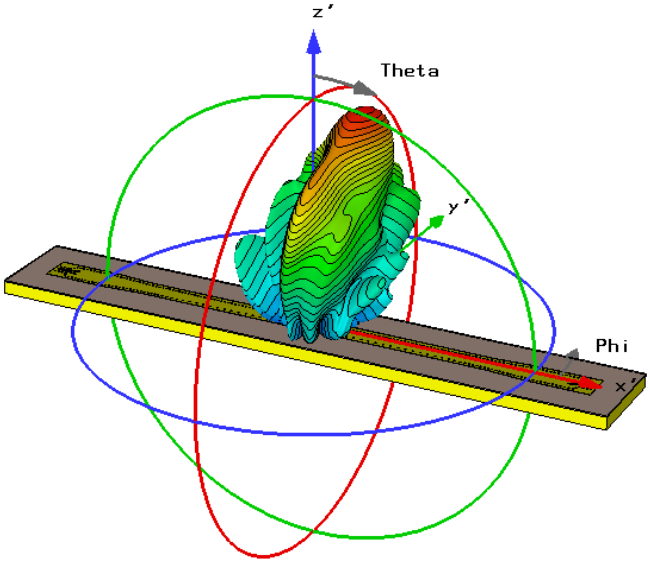

Fig. 6. Simulated 3D radiation pattern of 1st LWA at 91GHz.

Experimental Results

Three prototypes corresponding to the antennas of Table 1 have been fabricated and tested. Taconic's TaclamPLUS was selected as a suitable substrate for the realization of mm-wave circuits [33]. The substrate thickness is 0.1mm with permittivity of 2.08 and loss tangent of 0.0008. The top etchable metallization is copper of thickness 18µm and the bottom ground plane is 3mm brass, which provides robust support for the structure.

The prototypes have been etched using standard photolithographic techniques. The given PCB parameters coupled with the restrictions imposed by both the etching process (70-80µm track width) and the ground-signal-ground (GSG) probe dimensions (150µm pitch) imposed a lowest realizable impedance of about 80Ohm. In order to excite the antennas, usually GCPW-SIW transitions are employed [34, 35]. In this paper custom GCPW-SIW transitions compatible with the technological restrictions have been designed to match a 50Ohm GSG probe to the SIW feeding the antenna. The layout of the transition together with the optimized dimensions is shown in Fig. 7. The simulated characteristics of the transition are presented in Fig. 8. The transition ensures return loss better than 20dB in the frequency band of interest. The transitions have been cascaded with the LWA as in Fig. 1 and their dimensions are fixed for all antenna prototypes. Photographs of the fabricated prototypes are shown in Fig. 9.

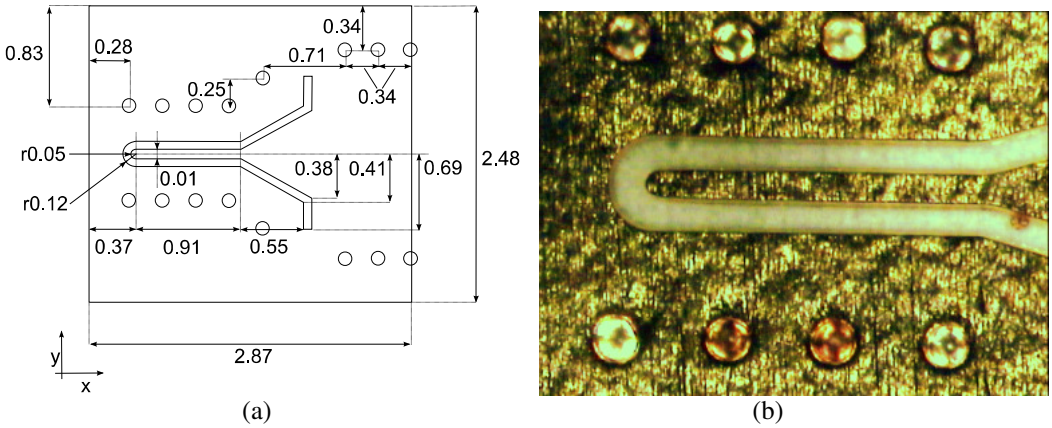

(a) (b)

Fig. 7. GCPW-SIW transition: (a) layout (the dimensions are in mm), (b) photo of a sample.

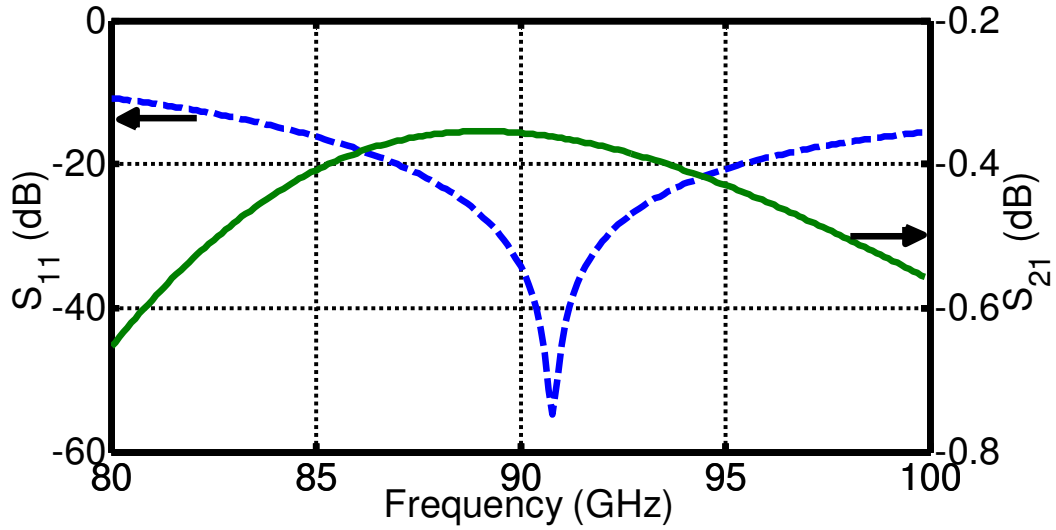

Fig. 8. Simulated S-parameters of the GCPW-SIW transition.

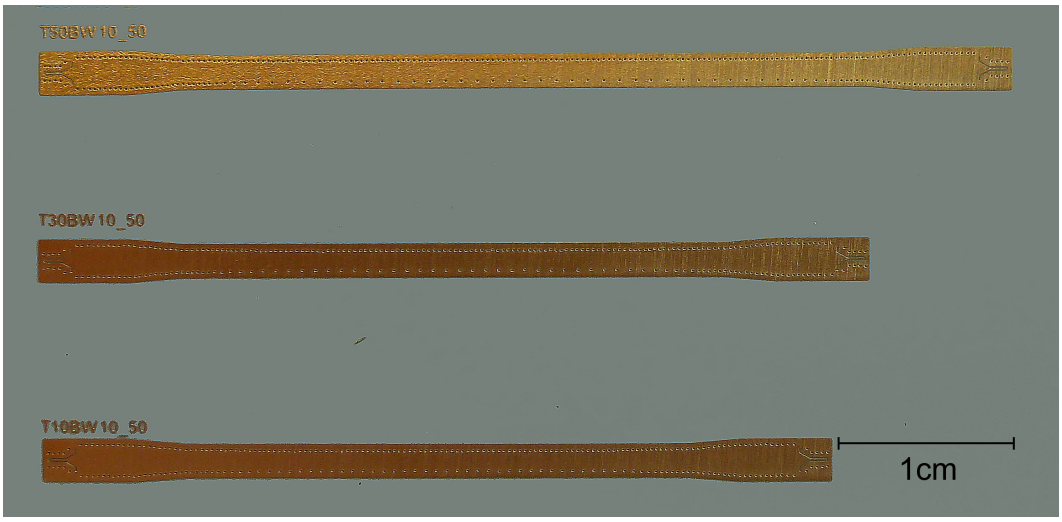

Fig. 9. Manufactured LWA antennas.

S-parameters

The antennas S-parameters were measured employing a Cascade millimeter-wave probe station with 50 ohm 150 µm GSG probes. The probes before each measurement were calibrated using an automated LLRM-procedure at the probe station and the calibration error was below 0.1 dB for the entire frequency range from 85 to 110 GHz. The results of the measurements and corresponding simulations for the 2nd antenna prototype of Table 1 are presented in Fig. 10. Good agreement between theory and experiment is observed, confirming the validity of the design. The antenna is well matched in the frequency band of interest. Measured return loss for the other two prototypes (not shown here for brevity) has shown S11<10dB at the operating frequencies, in good agreement with the simulation predictions.

All three designs present insertion losses below -10dB in the 85-100GHz band, thus confirming that the designed leakage rate lets a small fraction of energy (below 10%) reach the output port. In order to estimate the antenna efficiency, Fig. 11 shows the total measured power loss as obtained by [36]:

$$P_{tl} = 1 - |S_{11}|^2 - |S_{21}|^2 \quad (3)$$

The dissipative loss have been calculated by subtracting the total measured power loss obtained with (3) from simulated S-parameters of a lossless structure from the absorbed power for simulated lossy structure. This has been achieved by running two simulations with appropriate

metal and dielectric parameters in the CST Microwave Studio with time domain solver. Since the numerical uncertainty is higher when operating with small numbers the loss estimation gives almost zero at 88-90GHz, see Fig. 11. At the other frequencies the more realistic values are obtained, which allows considering the result as a fair approximation of the dissipative loss and use it for estimation of the radiated power.

The radiated power has been estimated by subtraction of the simulated dissipative losses from measured total power loss, this figure results in radiation efficiency in excess of 89% for the entire scanning bandwidth (88-94GHz), as also shown in Fig. 11, in good agreement with the theoretical estimation. This result confirms the success in obtaining the specified high efficiency. The efficiency can degrade slightly due to the surface wave generation. The issue was studied in [36] for wide microstrip line LWA which has similar radiation mechanism. It was shown that for similar dielectric properties and line width to substrate thickness ratios the content of spatial wave radiation exceeds 90% for the scanning angles we target. If this figure is factored in the efficiency obtained above, one arrives at estimated radiation efficiency of 80%.

More rigorous calculation of the efficiency would require directivity and gain measurements [37]. The former requires a full 3D radiation pattern scan on a spherical grid and could not have been performed with available instruments. The gain however was measured with a two-antenna setup, as the antenna under test and a 10dB standard horn were measured. With this method the gain of 9dB at 91GHz was obtained for the 2nd LWA. By comparison with the simulated directivity of 10dB, see Fig. 4, one can estimate the efficiency as 79%, which gives us similar value to the one obtained above.

For frequencies below the leaky scanning regime (f<88GHz), the reactive cut-off region of the SIW imposes high mismatch and thus low radiation efficiency. Similarly, the efficiency decreases for frequencies above 98GHz, due to the drop of the leakage rate associated to the transition from leaky to bound wave [36]. Similar results were obtained for the other two antennas, thus demonstrating the capacity of the proposed SIW LWA technology to design electrically-large, highly-efficient scanning antennas in the mm-wave frequency range.

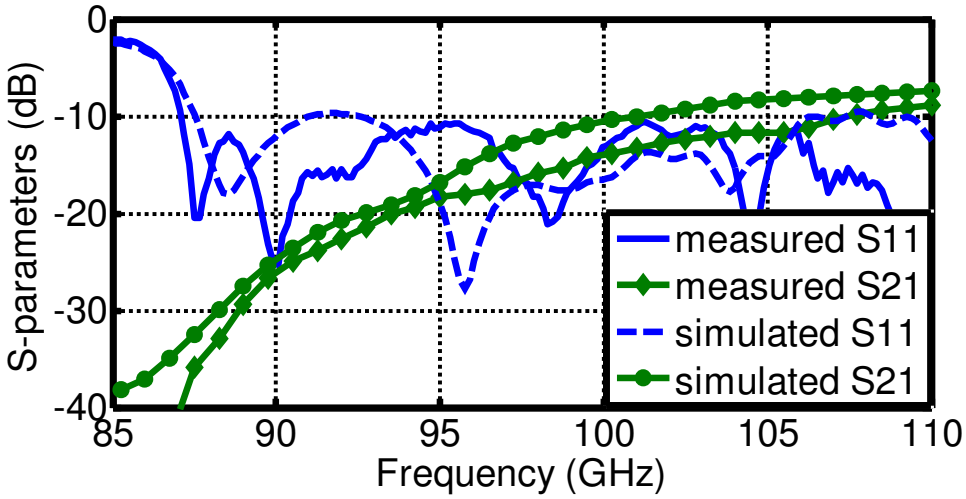

Fig. 10. S-parameters of the 2nd LWA.

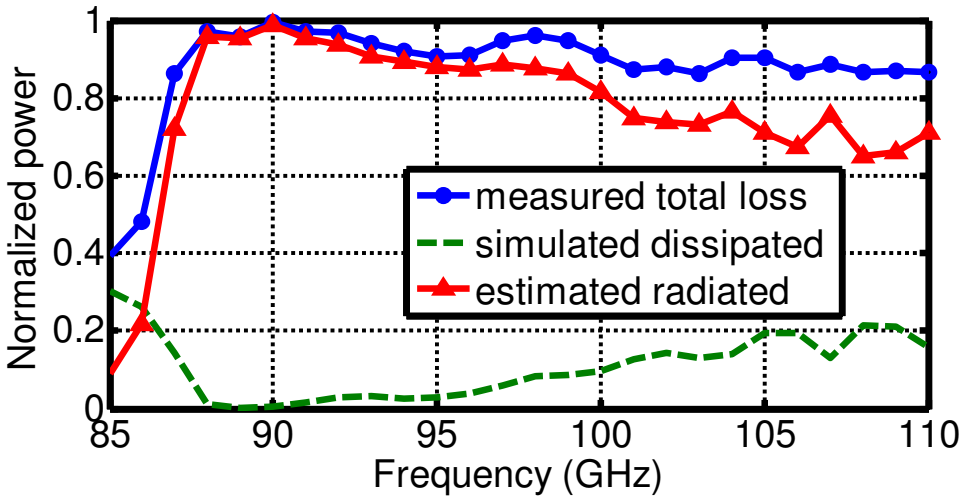

Fig. 11. Total loss, radiated and dissipated power of the 2nd LWA.

Radiation Pattern

Radiation pattern measurements were performed in an anechoic chamber. The board with the samples and the probe with holder were attached to a plastic fixture, shown in Fig. 12, which allows the setup to be rotated with a conventional positioner. The fixture ensures direct access to antennas through a coupling probe. The setup is liable to some interference towards endfire direction due to the probe with holder obstructing the line of sight between transmitting horn antenna and antenna under test. However, for directive antennas, this is not significantly affecting the main lobe as the antennas are placed so that the main beam points in opposite direction from the probe. The comparison of simulated and measured radiation patterns for all the antennas at different frequencies as measured with this setup is given in Fig. 13, Fig. 14 and Fig. 15.

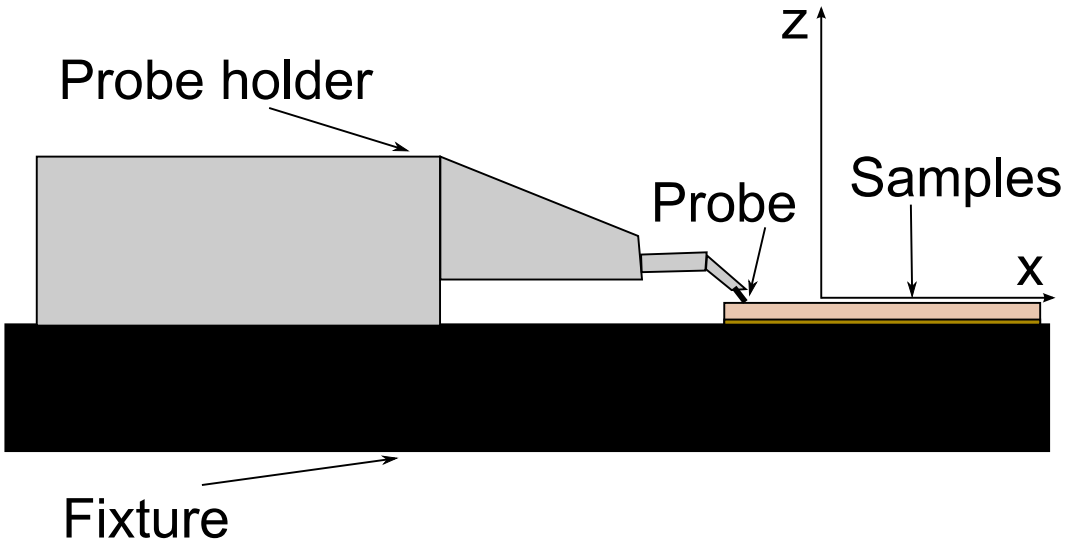

Fig. 12. Radiation pattern measurement fixture.

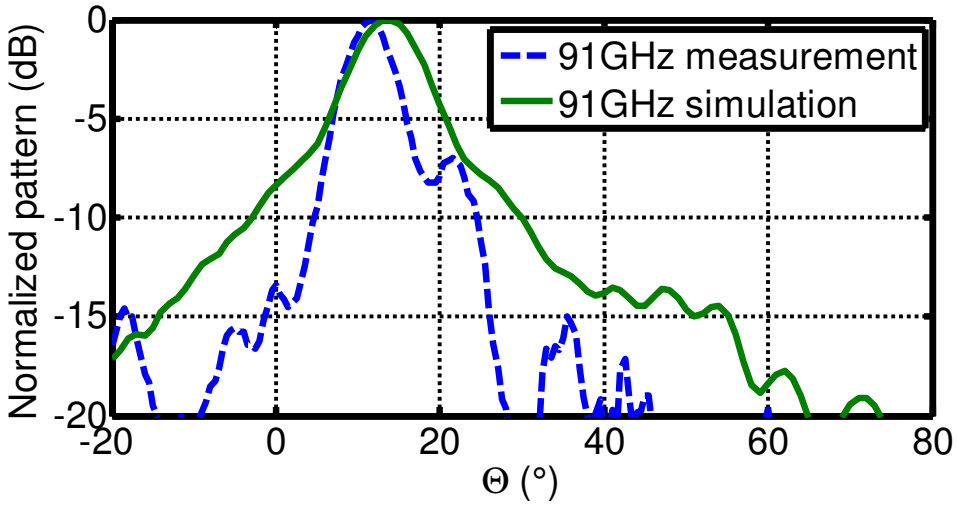

Fig. 13.Radiation pattern of 1st antenna at 91GHz.

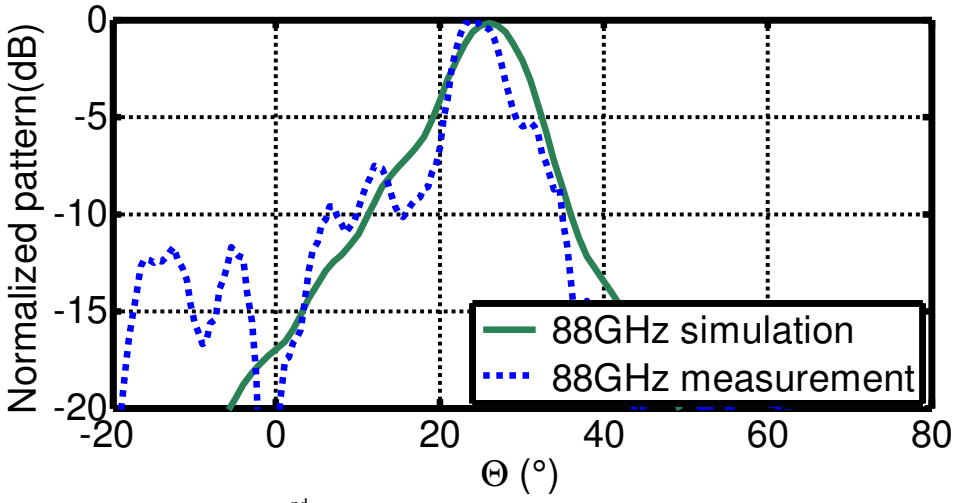

Fig. 14.Radiation pattern of 2nd antenna at 88GHz.

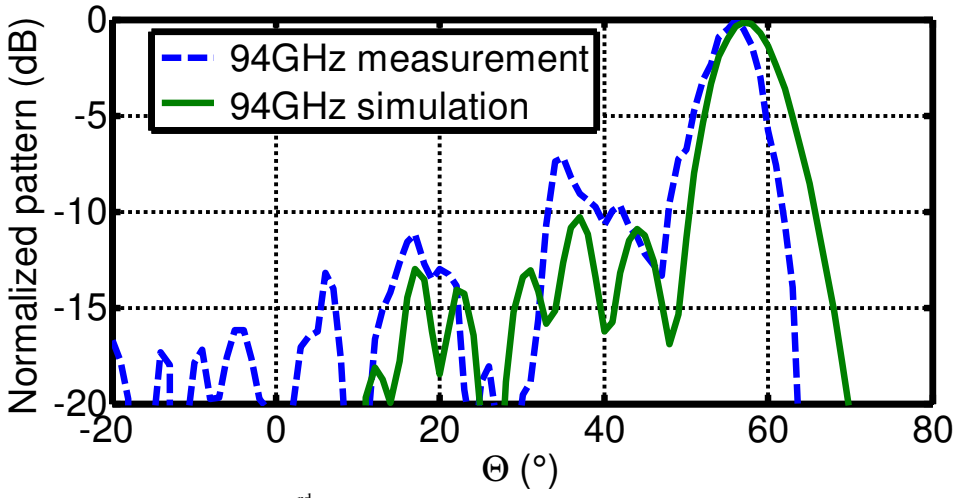

Fig. 15. Radiation pattern of 3rd antenna at 94GHz.

As one can see there is a good agreement between the simulated and the measured radiation patterns. Some deviation and squint of the measured beam in comparison with the simulation can be attributed to the manufacturing tolerances. In order to demonstrate the coverage of the elevation angle range, all measured radiation patterns are gathered in Fig. 16. The measurements have been

performed in 88-94GHz frequency range. From this figure it can be seen that the elevation angles from 11°-56° are covered by the set of the three antennas. Some discrepancies in the sidelobes are attributed to the fixture interference and could not be avoided with the available measurements facilities.

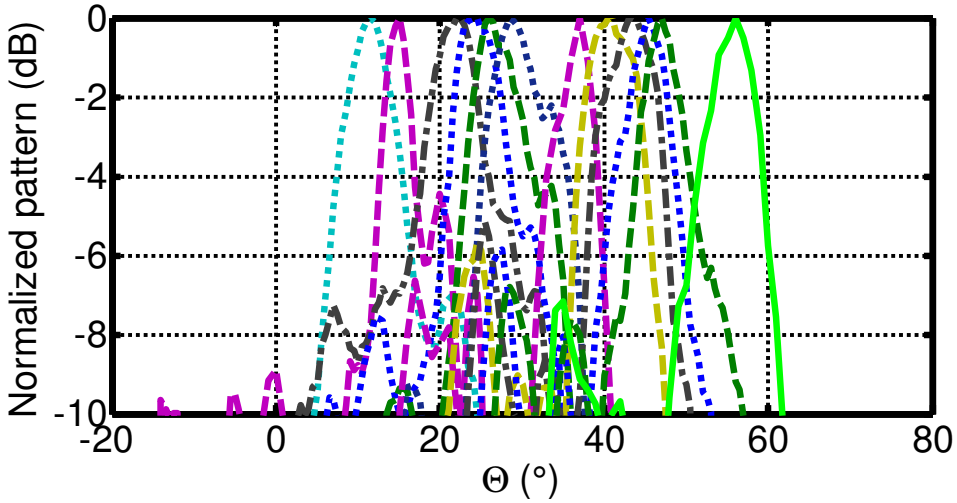

Fig. 16. Measured multi-sector radiation pattern of the 3-antenna setup.

Conclusion

A novel W-band hybrid wide-angle frequency-scanning SIW leaky-wave antenna architecture has been presented. Three antenna prototypes suitable for this architecture have been designed in SIW technology. The ensemble of the three antennas covers elevation angles from 13° to 55° by frequency scanning within a 6.5% bandwidth with an approximately constant 10° beamwidth. Prototypes have been fabricated and tested. Good agreement between the simulated and experimental results has been obtained. Coverage of elevation angles between 11°-56° has been demonstrated in the entire scanning region.

The compatibility with PCB technology and wide elevation scanning capability within a narrow frequency band make the proposed W-band antennas an attractive solution for intelligent mobile sensing and communications applications.

Acknowledgments

The work was partly supported by the FP7 GigaRadio Marie Curie project (IAPP/2008/230652) and the Leverhulme Trust Research Project Grant F/00 203/U-Phase Conjugate Wireless Communication. The authors appreciate assistance of Mr Jim Francey of OptiPrint AG with manufacturing of the antennas and advice on TaclamPLUS material properties by Mr Manfred Huschka of Taconic ADD.

References

1. Sturm C, Wiesbeck W (2011) Waveform Design and Signal Processing Aspects for Fusion of Wireless Communications and Radar Sensing. Proceedings of the IEEE 99(7):1236–1259
2. Groll HP, Detlefsen J (1996) History of automotive anticollision radars and final experimental results of a mm-wave car radar developed on the Technical University of Munich. Proceedings of International Radar Conference. Publishing House of Electron. Ind, Beijing, pp 13–17

3. Chou Y, Lin S, Chung S (2002) Analysis of a grating metal structure with broad back-scattering field pattern for applications in vehicle collision avoidance system. IEEE Transactions on Vehicular Technology 51(1):194–199
4. Pollard BD, Sadowy G, Moller D, Rodriguez E (2003) A millimeter-wave phased array radar for hazard detection and avoidance on planetary landers. IEEE Aerospace Conference Proceedings. IEEE, Pasadena, pp 1115–1122
5. Van Caekenberghe K, Brakora KF, Sarabandi K (2007) A 94 GHz OFDM Frequency Scanning Radar for Autonomous Landing Guidance. IEEE Radar Conference Proceedings. IEEE, Boston, pp 248–253
6. Jung Y-B, Eom S-Y, Jeon S-I (2010) Novel Antenna System Design for Satellite Mobile Multimedia Service. IEEE Transactions on Vehicular Technology 59(9):4237–4247
7. Appleby R, Anderton RN, Thomson NH, Jack JW (2004) The design of a real-time 94-GHz passive millimetre-wave imager for helicopter operations. In: Carapezza EM, Driggers RG, Kamerman GW, et al (eds) Proceedings of the SPIE. London, pp 38–46
8. Zhang YP, Liu D (2009) Antenna-on-Chip and Antenna-in-Package Solutions to Highly Integrated Millimeter-Wave Devices for Wireless Communications. IEEE Transactions on Antennas and Propagation 57(10):2830–2841
9. Appleby BR, Anderton RN (2007) Millimeter-Wave and Submillimeter-Wave Imaging for Security and Surveillance. Proceedings of the IEEE 95(8):1683–1690
10. Akkermans JAG, Herben MHAJ, Van Beurden MC (2009) Balanced-Fed Planar Antenna for Millimeter-Wave Transceivers. IEEE Transactions on Antennas and Propagation 57(10):2871–2881
11. Costa JR, Lima EB, Fernandes CA (2009) Compact Beam-Steerable Lens Antenna for 60-GHz Wireless Communications. IEEE Transactions on Antennas and Propagation 57(10):2926–2933
12. Thornton J, Gregson S, Gray D (2010) Aperture blockage and truncation in scanning lens-reflector antennas. IET Microwaves, Antennas & Propagation 4(7):828–836
13. Hirokawa J, Ando M, Goto N, Takahashi N, Ojima T, Uematsu M (1995) A single-layer slotted leaky waveguide array antenna for mobile reception of direct broadcast from satellite. IEEE Transactions on Vehicular Technology 44(4):749–755
14. Ettorre M, Sauleau R, Le Coq L (2011) Multi-Beam Multi-Layer Leaky-Wave SIW Pillbox Antenna for Millimeter-Wave Applications. IEEE Transactions on Antennas and Propagation 59(4):1093–1100
15. Feng Xu, Ke Wu, Xiupu Zhang (2010) Periodic Leaky-Wave Antenna for Millimeter Wave Applications Based on Substrate Integrated Waveguide. IEEE Transactions on Antennas and Propagation 58(2):340–347
16. Cheng YJ, Hong W, Wu K, Fan Y (2011) Millimeter-Wave Substrate Integrated Waveguide Long Slot Leaky-Wave Antennas and Two-Dimensional Multibeam Applications. IEEE Transactions on Antennas and Propagation 59(1):40–47
17. Jackson DR, Williams JT (2005) 2-D periodic leaky-wave Antennas-part II: slot design. IEEE Transactions on Antennas and Propagation 53(11):3515–3524
18. Gomez-Tornero JL (2011) Unusual tapering of leaky-wave radiators and their applications. Proceedings of the 5th European Conference on Antennas and Propagation (EUCAP). Rome, pp 821–824
19. Garcia-Vigueras M, Gomez-Tornero JL, Goussetis G, Weily AR, Guo YJ (2011) 1D-Leaky Wave Antenna Employing Parallel-Plate Waveguide Loaded With PRS and HIS. IEEE Transactions on Antennas and Propagation 59(10):3687–3694
20. Zhang M, Hirokawa J, Ando M (2011) An E-Band Partially Corporate Feed Uniform Slot Array With Laminated Quasi Double-Layer Waveguide and Virtual PMC Terminations. IEEE Transactions on Antennas and Propagation 59(5):1521–1527
21. Ando M, Zhang M, Lee J, Hirokawa J (2010) Design and Fabrication of Millimeter Wave Slotted Waveguide Arrays. Proceedings of the 4h European Conference on Antennas and Propagation (EuCAP). Rome, pp 1–6
22. Martinez-Ros AJ, Gomez-Tornero JL, Goussetis G (2012) Planar Leaky-Wave Antenna With Flexible Control of the Complex Propagation Constant. IEEE Transactions on Antennas and Propagation 60(3):1625–1630
23. Yu Jian Cheng, Wei Hong, Ke Wu (2010) Millimeter-Wave Half Mode Substrate Integrated Waveguide Frequency Scanning Antenna With Quadri-Polarization. IEEE Transactions on Antennas and Propagation 58(6):1848–1855
24. Huang M, Xu S, Pan Y (2008) Investigation on a Novel Leaky Wave Antenna with Double Radiation Beam Composed of Left-handed Slab Loaded Hybrid Waveguide using Planar Technology. Journal of Infrared, Millimeter, and Terahertz Waves 30(2):117–127

25. Thian M, Buchanan NB, Fusco V (2011) Ultrafast Low-Loss 40–70 GHz SPST Switch. IEEE Microwave and Wireless Components Letters 21(12):682–684
26. Deslandes D, Wu K (2001) Integrated microstrip and rectangular waveguide in planar form. IEEE Microwave and Wireless Components Letters 11(2):68–70
27. Bozzi M, Perregrini L, Wu K, Arcioni P (2009) Current and Future Research Trends in Substrate Integrated Waveguide Technology. Radioengineering 18(2):201–209
28. Goldstone L, Oliner A (1959) Leaky-wave antennas I: Rectangular waveguides. IRE Transactions on Antennas and Propagation 7(4):307–319
29. Pozar DM (1997) Microwave Engineering, 2nd ed. John Wiley & Sons
30. Xu F, Wu K (2005) Guided-wave and leakage characteristics of substrate integrated waveguide. IEEE Transactions on Microwave Theory and Techniques 53(1):66–73
31. Garcia-Vigueras M, Gomez-Tornero JL, Goussetis G, Weily AR, Guo YJ (2011) Enhancing Frequency-Scanning Response of Leaky-Wave Antennas Using High-Impedance Surfaces. IEEE Antennas and Wireless Propagation Letters 10(3):7–10
32. Martinez-Ros A, Gomez-Tornero JL, Quesada-Pereira F, Alvarez-Melcon A (2011) Transverse resonance analysis of a planar leaky wave antenna with flexible control of the complex propagation constant. IEEE International Symposium on Antennas and Propagation (APSURSI). IEEE, pp 1289–1292
33. Zelenchuk DE, Fusco V, Goussetis G, Mendez A, Linton D (2012) Millimeter-Wave Printed Circuit Board Characterization Using Substrate Integrated Waveguide Resonators. IEEE Transactions on Microwave Theory and Techniques 60(10):3300–3308
34. Patrovsky A, Daigle M (2007) Millimeter-wave wideband transition from CPW to substrate integrated waveguide on electrically thick high-permittivity substrates. 2007 European Microwave Conference. IEEE, pp 138–141
35. Deslandes D, Wu K (2005) Analysis and design of current probe transition from grounded coplanar to substrate integrated rectangular waveguides. IEEE Transactions on Microwave Theory and Techniques 53(8):2487–2494
36. Lin Y-D, Sheen J-W (1997) Mode distinction and radiation-efficiency analysis of planar leaky-wave line source. IEEE Transactions on Microwave Theory and Techniques 45(10):1672–1680
37. Balanis CA (1997) Antenna Theory: Analysis and Design, 2nd ed. 960